Int. J. Multiphase Flow Vol. 11, No. 2, pp. 189–199, 1985
Printed in the U.S.A.

0301-9322/85 $3.00 + .00

EXPERIMENTS ON SEDIMENTATION BENEATH DOWNWARD-FACING INCLINED WALLS

UWE SCHAFLINGER
Institut für Strömungslehre und Wärmeübertragung, Technische Universität Wien, Vienna, Austria

(*Received* 6 *May* 1984; *in revised form* 9 *July* 1984)

Abstract—It has been known since Boycott (1920) that sedimentation rates can be several times higher within inclined walls than in vertical vessels. Beneath the downward-facing inclined wall a thin boundary-layer of clear liquid is formed with an upward velocity. Mass continuity brings about the observed effect. Ponder (1925), and Nakamura & Kuroda (1937) proposed a global kinematic model without any detail of the flow field to predict the sedimentation rate. Recently, two asymptotic theories for describing the flow field became available. The investigation by Acrivos & Herbolzheimer (1979) requires both Re^2/Gr and Re^4/Gr to be small, with Re being a sedimentation Reynolds number and Gr a sedimentation Grashof number. The analysis due to Schneider (1982) is valid for small values of Re^2/Gr and large values of Re^4/Gr. This paper presents experimental sedimentation data in a symmetrical, roof-shaped vessel. The experiments with spherical glass beads in a variable mixture of glycerine and water cover the whole parameter range from very small to very large values of Re^4/Gr. Therefore, both theories could be verified. In the case of small values of Re^4/Gr, strong waves beneath the downward-facing wall were observed and graphically evaluated in order to find a basis for further theoretical approach. Furthermore, an upward flow of particles in a sublayer of the boundary-layer leads to protruding "horns" and an oscillation of the originally horizontal discontinuity separating the suspension from the clear liquid. The measured particle distribution and deviations from a monodispersed suspension seems to be a possible explanation for this effect, which is investigated theoretically in a separate paper (Schaflinger 1984). A further experimental shortcoming, the shallow depth of the settling vessel, that was necessary for an optoelectronic measuring of the actual volume fraction solids within the bulk, may affect the convective motion when the sedimentation Reynols number is small. However, in this case the experimental data are in conformity with the theoretical predictions which do not consider the influence of wall friction on the sedimentation behaviour.

1. INTRODUCTION

Many investigators studied the phenomenon of the "Boycott effect" for a variety of suspensions and reported that an increase in the sedimentation rate could thereby be achieved. A kinematic model based on experimental observations which led to a quantitative prediction for the sedimentation rate was presented by Ponder (1925) and independently by Nakamura & Kuroda (1937) and will be referred to henceforth as the PNK model. Previous experiments (Kinosita 1949, Pearce 1962, Graham & Lama 1963, Oliver & Jenson 1964, Vohra & Ghosh 1971 and Zahavi & Rubin 1975) have demonstrated that an acceptable conformance with the PNK model depends on sedimentation conditions. Hill *et al.* (1977) produced numerical solutions of the two-phase flow equations for a very dilute suspension of particles that settle with a predetermined velocity relative to the fluid. These authors extrapolated their results and concluded that the PNK model correctly expressed the sedimentation rate in the dual limit of a sedimentation Grashof number Gr and a sedimentation Reynolds number Re, whereby $Gr \to \infty$ and $Re \to 0$. The two dimensionless groups are defined as follows:

$$Gr = H^3 g \alpha_0 (\rho_2 - \rho_1)/\rho_1 \nu_1^2, \quad [1]$$

$$Re = HU/\nu_1, \quad [2]$$

where H is a characteristic height of the suspension, α_0 is the initial volume fraction of solids, g is the gravitational constant, ρ is the density and ν is the kinematic viscosity. The index 1 refers to the clear fluid and the index 2 to the solid particles. U is the settling velocity of an

individual particle given, for instance, by Stokes' law

$$U = d^2(\rho_2 - \rho_1)g/18\rho_1\nu_1, \qquad [3]$$

where d is the diameter of the spherical particles.

Quite recently, two asymptotic theories (Acrivos & Herbolzheimer 1979 and Schneider 1982) for describing the total flow field became available. The investigation by Acrivos & Herbolzheimer requires both Re^2/Gr and Re^4/Gr to be small. They proved that the sedimentation rate can be predicted by the PNK model, from which we derive a formula for a roof-shaped vessel, written in dimensionless variables

$$z_0^2 - h^2 = \frac{\alpha_s - \alpha_0}{\alpha_0}\left\{1 - \left[1 - \frac{f(\alpha_0)}{\alpha_s - \alpha_0}t\right]^2\right\}, \qquad [4]$$

with z_0 being the coordinate in direction of settling and h the initial height of the suspension. Both lengths are referred to H, the height of the vessel, and t is referred to the characteristic time H/U (figure 1). To distinguish between dimensionless and dimensional variables, the latters are marked with a bar in the following test.

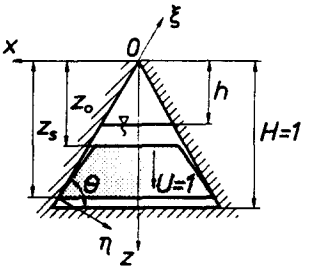

Figure 1. Definition of variables.

Furthermore α_s is the particle concentration in the sediment (packed bed). For hard spheres α_s is known to be about 0.6. The function $f(\alpha)$ must be determined by suspension mechanics or experiments. In our case an empirical correlation of the power-law form

$$f(\alpha) = \alpha(1 - \alpha)^n \qquad [5]$$

is used. According to Richardson & Zaki (1954), cf. also Wallis (1969, p. 178), the value $n = 4.7$ gives good results. Equation [4] is incorrect for a limited range of α_0, in the case when centred waves within the suspension appear (Schneider 1982). The analysis by Schneider is valid for small values of Re^2/Gr and large values of Re^4/Gr and leads to a two- or three-dimensional kinematic wave theory for the bulk and in contrast to that of Acrivos & Herbolzheimer to the possibility of a subsequent insert of the clear liquid boundary layer, where, in a first approximation, the flow is inviscid and quasisteady. The solutions presented by Schneider are for the whole range of the initial volume fraction $0 < \alpha_0 < \alpha_s$.

The paper by Acrivos & Herbolzheimer (1979) and Schneider (1982) will henceforth be referred to quite frequently and therefore, will be labelled for brevity AH, and S, respectively.

This paper provides experimental sedimentation data in a symmetrical, roof-shaped vessel. The experiments cover the whole parameter range from very small to very large values of Re^4/Gr with a constant initial volume fraction α_0 of spherical glass beads in a variable mixture of glycerine and water. Therefore, both theories, AH and S, could be verified. For this purpose the experiment's results of the measured widths of the clear liquid boundary layer beneath the downward-facing inclined wall are compared with the theoreti-

cal predictions. In boundary-layer coordinates (ξ, η) with ξ denoting the coordinate along the downward-facing surface and η the coordinate normal to it, both referred to H, the dimensionless boundary-layer thickness δ_{AH}, according to AH, becomes

$$\delta_{AH} = \left(3\frac{f(\alpha_0)}{\alpha_0}\xi \operatorname{ctg}\theta\right)^{1/3}\left(\frac{Re}{Gr}\right)^{1/3} \qquad [6]$$

and the dimensionless boundary-layer thickness δ_s, according to S, becomes

$$\delta_S = \frac{(2\sin\theta)^{1/2}}{\tan\theta}\frac{f(\alpha_0)}{\alpha_0}\xi^{1/2}\frac{Re}{Gr^{1/2}}, \qquad [7]$$

where θ denotes the inclination angle between the horizontal and the downward-facing wall.

Although, according to S the tangential velocity is linearly distributed across the boundary layer and AH calculated a parabolic velocity profile within the upstreaming clear liquid, a Reynolds number Re_b for the clear liquid boundary layer is independent of the above-mentioned theories and becomes

$$Re_b = Re\frac{f(\alpha_0)}{\alpha_0}\xi\cos\theta, \qquad [8]$$

where Re is the sedimentation Reynolds number defined by [2]. Hence we obtain a critical Reynolds number $\hat{Re}_b$ for the observed wave formation under the inclined wall when $\hat{\xi}$ is the inception distance. A linear stability analysis by Herbolzheimer (1983), following the paper by AH for the limited range of Re^2/Gr and Re^4/Gr, leads to an asymptotic solution for long waves and corresponds well with his own experiments. The conclusions by Herbolzheimer are consistent with our experiments as well, whereas an analysis due to Prasad (1985) conflicts with the measured data.

2. EXPERIMENTAL SETUP

The object of the experimental work was to check the theories due to AH and S. Thus, the experiments require a symmetrical, roof-shaped vessel with a constant initial volume fraction of solids, which were spherical, blue coloured glass beads with a nominal mean diameter $d = 125\ \mu$m and a density $\rho_2 = 2790\ \text{kg/m}^3$. The sedimentation fluid that was used was a variable mixture of glycerine and distilled water with a dynamic viscosity between $\eta = 1$ mPas (clear water) and $\eta = 85$ mPas (clear technical glycerine), and with a density between $\rho_1 = 1000\ \text{kg/m}^3$ and $\rho_2 = 1230\ \text{kg/m}^3$. Thus, the whole parameter range for both theories (AH and S) could be covered in a vessel with height $\overline{H} = 463$ mm. Figure 2 shows

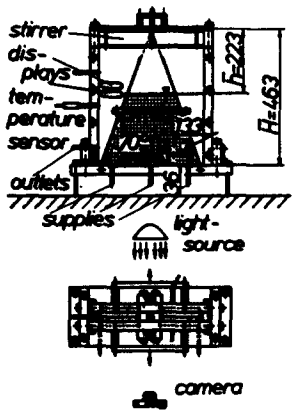

Figure 2. Experimental setup.

the design of the settling tank with its typical dimensions. For visual observations, the front plates were made of transparent acrylic-plastic with a thickness and a spacing of 30 mm in each case. These permitted the inclined walls to be halved so that each component could be retracted in guide slots. In this manner it was possible to produce a homogeneous suspension in the same way that it is usually done in cylindrical vessels with a flat stirrer. In our case we used two parallel stirrers that had a staggered row of holes and were guided and fixed in the cap of the vessel. The advantage of this design was that all experiments could be started with well-defined initial conditions. Antileak seals separated the flow within the inclined walls precisely from the flow outside. The flow outside the inclined walls was not of interest to the experiment.

An optoelectronic measuring device indicated the local volume fraction of solids during an experimental process. Figure 2 also shows where the sensor was attached. A balance unit enabled the actual value of concentration to be directly read on a digital display which was mounted on the left side of the front plate. The spacing of the front plates and the range of the volumetric concentration of solids were restricted by the conditions of the physical properties of the measuring system, in particular by the nonlinear function between the concentration and the light permeability of the suspension, as well as by the nonlinear function between the concentration and the light being incident on the phototransistor used and its collector current. The assumption that the influence of wall friction should be negligibly small requires a separation time which is very short compared to that for vorticity diffusion. This leads to the following restriction:

$$Re\left(\frac{b}{\overline{H}}\right)^2 \gg 1, \qquad [9]$$

with b being the spacing distance. The kinematic wave theory (S) required a large sedimentation Reynolds number ($Re \sim 10^4$) for our experiments. With a spacing distance of $b = 30$ mm and a vessels height of $\overline{H} = 463$ mm, condition [9] was satisfied. In the range of $Re = O(1)$ (AH) the influence of the shallow depth of the settling vessel on the convective motion within the tank should be taken into account. In spite of this experimental shortcoming the sedimentation rate, as well as the boundary-layer-thickness are in good agreement with the two-dimensional theoretical predictions. With the chosen spacing distance an optimal accuracy of the measuring equipment ranged between $\alpha = 0.005$ and $\alpha = 0.022$.

Afflux and flowing off supplies for the clear liquid were mounted in the bottom of the tank, whereby a sieve plate prevented the solid particles from running off. Thus, the initial concentration could be kept constant by changing the fluid quickly. Several outlet pipes arranged in different heights on the left vertical wall served the purpose of particle classification, because both theories AH and S require a monodispersed suspension. A digital time display, located below the concentration display, made a photographic documentation of the experiments possible. The first picture at time $t = 0$ was taken, when the inclined walls were just closed.

Because the influence of temperature on fluid properties was not to be studied, the temperature was controlled and kept constant with 21 °C.

3. EXPERIMENTAL PROCEDURE

Before starting the actual experiments the drift-flux relation and the particle distribution were determined from settling heights and sedimentation rates, respectively. Figure 3 compares the measured values of the drift flux with the relation according to [5]. With $n = 4.7$ the experimental data conforms quite well with the empirical counterpart. Figure 4 shows the measured particle distribution. The deviations of a monodispersed suspension

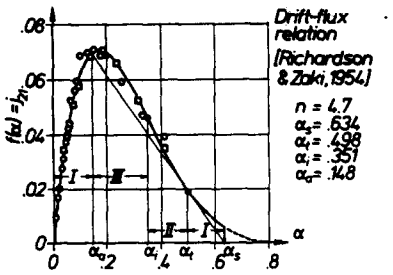

Figure 3. Comparison between the experimental drift-flux relation according to Richardson and Zaki (1954) and the experiment: O glycerine—ethanol $\rho_1 = 896.25$ kg/m^3, $\rho_2 = 2910.0$ kg/m^3, $d = 105$ μm, $\eta = 2.8$ mPas; □ glycerine—water $\rho_1 = 1191.0$ kg/m^3, $\rho_2 = 2790.0$ kg/m^3, $d = 125$ μm, $\eta = 19.5$ mPas. Classification I, II, and III according to Wallis (1969, pp. 191–194). $\alpha_{s,i,s}$ according to Schneider (1982).

could be a possible explanation for effects that were observed. This will be discussed in section 4.4.

A suspension filling level of $\bar{h} = 223$ mm with a quantity of 100-g solids yielded an initial volume fraction of $\alpha_0 = 0.014$, which was kept constant for all experiments. To cover the whole parameter range from very small values to very large values of Re^4/Gr seven typical experiments were chosen and are represented in table 1 along with the corresponding values of parameters, whereby $\epsilon_1 = Re/Gr^{1/2}$ and $\epsilon_2 = Gr^{1/4}/Re$. The ninth row of table 1 shows the order of magnitude of the relative error with respect to the corresponding theory.

The procedure started with clear technical glycerine and a dynamic viscosity of $\eta = 85$ mPas for the first sedimentation run. A discharge of the mixture fluid and charge of distilled water to adjust the next decreasing value of fluid viscosity led to the runs following in order. All sedimentation runs were documented both as series of single pictures and as substandard cine films.

4. EXPERIMENTAL RESULTS

4.1. *Sedimentation rate and settling time*

In the limiting case of a very dilute suspension, i.e. $\alpha_0 \to 0$, we deduce the sedimentation rate from [4]

$$z_0 = (h^2 + 2t)^{1/2}, \qquad [10]$$

from which the total settling time, exactly when $z_0 = 1$,

$$t_s = \tfrac{1}{2}(1 - h^2) \qquad [11]$$

is predicted.

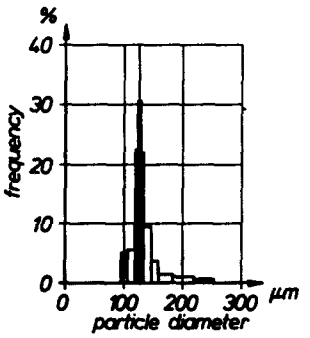

Figure 4. Particle size distribution.

Table 1. Parameters of the experiments

dyn. viscosity of the fluid η [mPas]	85	16	11.5	8	4.5	2	1
density of the fluid ρ[kg/m³]	1230	1176	1157,5	1132	1101	1025	1000
	range of A and H theory			transition range		range of S theory	
Re	1	29	56	115	360	1783	7057
Gr	3.6×10^{6}	10^{8}	1.9×10^{8}	3.8×10^{8}	1.2×10^{9}	6.5×10^{9}	2.4×10^{10}
$(Re/Gr)^{1/3}$	0.007						
ϵ_1	5.2×10^{-4}	2.9×10^{-3}	4×10^{-3}	5.9×10^{-3}	1.3×10^{-2}	2.2×10^{-2}	0.05
ϵ_2	43.5	3.4	2.9	1.2	0.5	0.2	0.05
error estimate	$0(\epsilon_2^{-4/3})$					$0(\epsilon_2)$	
	0.006	0.2	0 .24			0.2	0.05
α_0	0.014						
ρ[kg/m³]	2790						
d[µm]	125						
H[mm]	463						
Θ	70°						

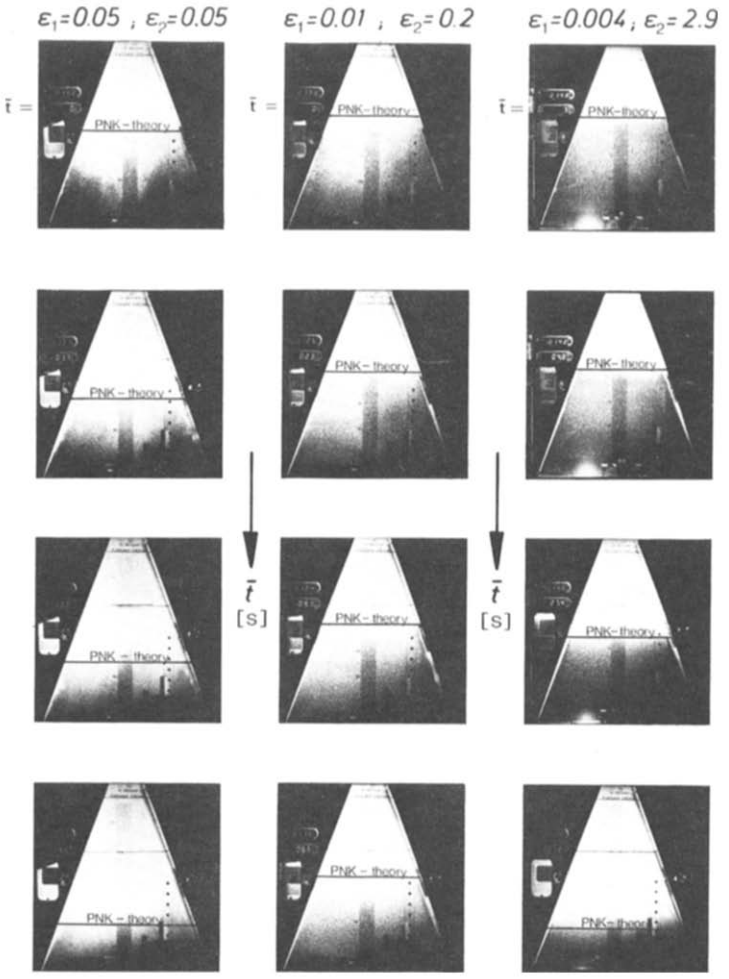

Figure 5. Sedimentation rate; comparison between PNK model and experiment.

Our experiments were conducted with an initial concentration $\alpha_0 = 0.014 \ll 1$ so that comparisons between the measured sedimentation rates and the results provided by [10] and [11] are justified. The evaluations are in agreement with the PNK formula [10] as shown in figure 5, where three typical experiments are represented for both theories (AH and S) and for the transition region. In the range of $\epsilon_2 < 1$ a strong upward flow of particles in a sublayer of the boundary layer leads to protruding "horns" and an oscillation of the originally horizontal interface, separating the suspension from the clear liquid. The latter is plotted in figure 6 for the case of $\epsilon_1 = 0.05$ and $\epsilon_2 = 0.05$ which is in the range of S. A possible physical explanation of the observed effects is given in section 4.4.

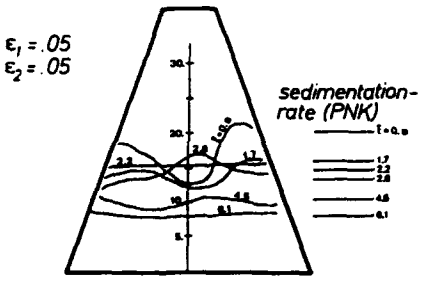

Figure 6. Oscillation of the interface suspension–clear liquid.

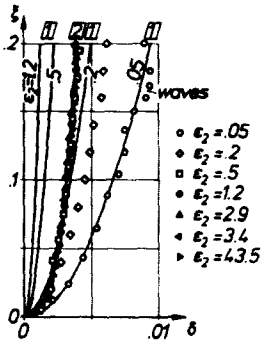

Figure 7. Boundary-layer thickness; comparison between theories and experiments. [1] Schneider (1982); [2] Acrivos and Herbolzheimer (1979).

4.2 *Boundary-layer thickness*

Dependent on ϵ_2 the predicted boundary-layer thickness obeys either the theory by AH [6], or S [7]. The comparison between the measured boundary-layer thickness and the calculations according to [6] and [7] leads to the following results (figure 7):

–The range of $\epsilon_2 \gg 1$ complies well with the solution developed by A and H.
–The whole transition region, where $\epsilon_2 = 0$ (1) is also determinated by [6], although the assumptions for the theory by AH are no longer valid.
–In the case of $\epsilon_2 \ll 1$ the experiments show that the boundary-layer thickness is in agreement with [7] derived by S. In this range strong waves beneath the downward-facing wall were observed, which complicated an unambiguous evaluation. Therefore, in figure 7 the coordinate ξ is limited to 0.2.

4.3 *Wave formation and growth*

Pearce (1962) mentioned in his paper that he observed a river of clear liquid ascending beneath the upper part of the tube wall, which was crooked and had many tributaries spreading into the suspension. Zahavi & Rubin (1975) noted that waves were formed on the suspension surface just under the inclined plane. In the experiments performed in our laboratory these phenomenons also appeared and could be evaluated in reference to the extensive documentation. In figure 8 the measured boundary layer is plotted versus the sedimentation time, whereby the height z_0 from [10] is associated with the coordinate

$$\xi = (1 - z_0)/\sin\theta. \qquad [12]$$

The evaluation of the observed wave growth during sedimentation leads to the following results:

–As the fluid viscosity increases, the amplitude decreases and no more waves appear when

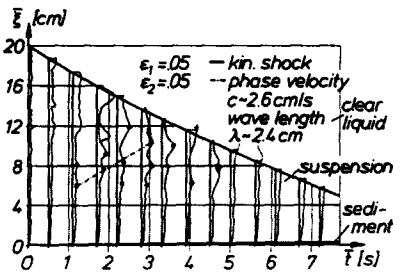

Figure 8. Measured boundary-layer thickness versus sedimentation time.

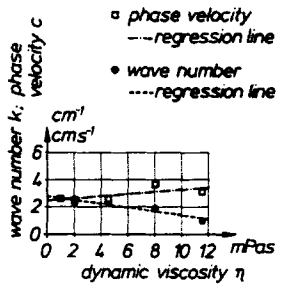

Figure 9. Experimental wave number k and phase velocity c versus the dynamic fluid viscosity.

$\eta > 11.5$ mPas. On the other hand, the wave length λ and the wave number $k = 2\pi/\lambda$, as well as the phase velocity c, are nearly constant within the measured range (figure 9).

–We obtain the critical Reynolds number $\hat{Re}_b$ from [8], which defines the Reynolds number for the boundary layer, with the observed inception distance $\hat{\xi}$ of the wave formation under the inclined wall. The experimental results show that $\hat{Re}_b$ is 100 times greater in the range of $\epsilon_2 \ll 1$ than in the range of $\epsilon_2 \gg 1$, where $\hat{Re}_b \sim 10$ (figure 10). The last value, as well as the measured wave numbers are in approximate agreement with the solutions of the linear stability analysis by Herbolzheimer (1983). When we transfer the results, given by Herbolzheimer, for $\theta = 70°$ and $\alpha_0 = 0.014$ in our diagram, we obtain the dashed line in figure 10, for which the regression line, resulting from the experimental data, is almost parallel. Thus we suppose that the wave mechanism is the same for all values of ϵ_2 and the basic ideas of Herbolzheimer may also be transferred to the investigations by S for a theoretical approach in this parameter range.

4.4 *Deformities of the interface between suspension and clear liquid*

Zahavi & Rubin (1975) noticed in their experiments that the upward movement of many small particles was caused by the clear liquid ascending under the inclined plane. All our experiments revealed an upstreaming sub-boundary layer, including particles as well. Subject to its high-flow velocity this layer was distinguishable particularly in the case of $\epsilon_2 \ll 1$. Thereby, the originally horizontal discontinuity, separating the suspension from the clear liquid, was deformed to protruding "horns" (figure 11) which gave rise to an oscillation of the interface (cf. section 4.1). This process is due to a pressure gradient in the horizontal direction which is maintained by a continuous flow of upstreaming particles. The particle distribution and deviations from a monodispersed suspension was considered in order to find a possible explanation for the observed effects. The free shear layer, developed and calculated in S, does not explain these phenomenons sufficiently. Within the parameter range, however, which satisfies the assumptions of AH's theory, there is a particle stream in

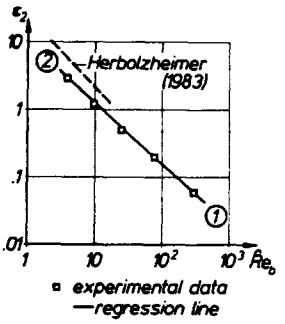

Figure 10. Critical boundary layer Reynolds number $\hat{Re}_b$ versus ϵ_2. ① Range of theory by Schneider (1982); ② range of theory by Acrivos & Herbolzheimer (1979).

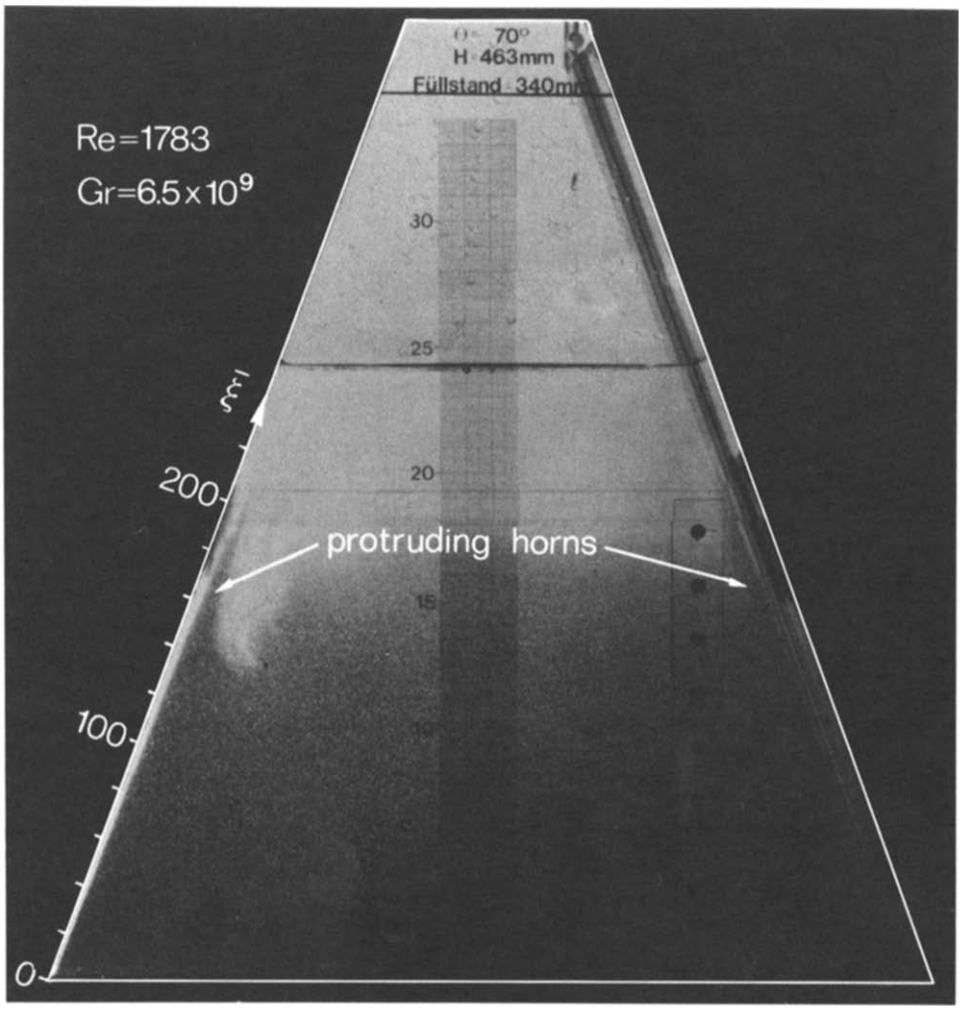

Figure 11. Observations of the flow.

the solution for the flow field included, since the tangential velocity has a maximum at the interface clear liquid suspension. Another paper (Schaflinger 1984) provides theoretical results on the influence of nonuniform particle size on the settling behaviour beneath downward-facing inclined walls. The derived solutions lead to a sub-boundary layer, which, given the conditions of the experiment, is within the observed magnitude of the upstreaming particle layer.

5. CONCLUSIONS

It may be concluded that in the presence of inclined walls the sedimentation rate can be predicted by the well-known PNK model (AH), when the range of an initial concentration is excluded where centered waves appear (S) and the packed bed on the bottom is taken into account. All our experiments that spread out over the whole parameter range from very small values to very large values of Re^4/Gr in order to verify both theories (AH and S) demonstrate that the settling rate concurs with the PNK model. As mentioned earlier, the experiments performed by Pearce (1962), showed that under certain sedimentation conditions the settling rates differ widely from a theoretical conclusion. The instabilities of the clear liquid boundary layer beneath the downward-facing wall as well as deviations of the monodispersed suspension could explain this phenomenon. Both lead to a remixing process of particles due to the high tangential velocity within the boundary layer. The evaluation of the observed wave formation and growth give rise to a critical Reynolds number which is in

accordance with a theoretical investigation on this subject by Herbolzheimer (1983). Because both curves in our diagram (figure 10) are almost parallel, we assume, that the wave mechanism is the same for all values of ϵ_2.

The observed sub-boundary layer of upstreaming particles is the subject of a theoretical paper investigating the influence of nonuniform particle size on the settling of particles beneath inclined walls (Schaflinger 1984).

As shown experimentally the thickness of the boundary layer is accurately predicted by AH for a wide range, which includes the transition range where the assumptions for this theory are no longer valid. When $\epsilon_2 \ll 1$ the thickness of the measured boundary layer is in accordance with the predicted values by S.

Acknowledgments—This work is an abridged version of the experimental section of the author's PhD thesis. The author should like to thank Professor Dr. W. Schneider for supervising this work and for many helpful comments. The experiments were supported by the Fonds zur Förderung der wissenschaftlichen Forschung, Projekt Nr. P4078.

REFERENCES

ACRIVOS, A. & HERBOLZHEIMER, E. 1979 Enhanced sedimentation in settling tanks with inclined walls. *J. Fluid Mech.* **92,** 435–457

BOYCOTT, A. E. 1920 Sedimentation of blood corpuscles. *Nature* **104,** 532.

GRAHAM, W. & LAMA, R. 1963 Sedimentation in inclined vessels. *Can. J. Chem. Eng.* **41,** 31–32.

HERBOLZHEIMER, E. 1983 Stability of the flow during sedimentation in inclined channels. *Phys. Fluids* **26,** 2043–2054.

HILL, W. D., ROTHFUS, R. R. & LI, K. 1977 Boundary-enhanced sedimentation due to settling convection. *Int. J. Multiphase Flow* **3,** 561–583.

KINOSITA, K. 1949 Sedimentation in tilted vessels. *J. Colloid. Interface Sci.* **4,** 525–536.

NAKAMURA, H. & KURODA, K. 1937 La cause de l'accélération de la vitesse de sédimentation des suspensions dans les récipients inclinés. *Keijo J. Med.* **8,** 256–296.

OLIVER, D. R. & JENSON, V. G. 1964 The inclined settling of dispersed suspensions of spherical particles in square-section tubes. *Can. J. Chem. Eng.* **42,** 191–195.

PEARCE, K. W. 1962 Settling in the presence of downward-facing surfaces. *Proc. 3rd Congr. Eur. Fed. Chem. Engng. Lond.* pp. 30–39.

PONDER, E. 1925 On sedimentation and rouleaux formation. *Quart. J. Exp. Physiol.* **15,** 235–252.

PRASAD, P. 1985 Waves at the interface of clear liquid and a mixture in a two phase flow. *J. Fluid Mech.* (in press).

RICHARDSON, J. F. & ZAKI, W. N. 1954 Sedimentation and fluidization: Part I. *Trans. Inst. Chem. Engrs.* **32,** 35–53.

SCHAFLINGER, U. 1984 Influence of nonuniform particle size on the settling beneath downward-facing inclined wall. *Int. J. Multiphase Flow.* (submitted).

SCHNEIDER, W. 1982 Kinematic wave theory of sedimentation beneath inclined walls. *J. Fluid Mech.* **120,** 323–346.

VOHRA, D. K. & GHOSH, B. 1971 Studies of sedimentation in inclined tubes. *Ind. Chem. Engng.* **13,** 32–40.

WALLIS, G. B. 1969 *One-dimensional Two-phase Flow.* McGraw Hill.

ZAHAVI, E. & RUBIN, E. 1975 Settling of solid suspensions under and between inclined surfaces. *Ind. Eng. Chem., Process Des. Develop.* **14,** 34–40.